Frontiers in Bioscience Landmark

Front. Biosci. (Landmark Ed) **2025**; 30(2): 27119
https://doi.org/10.31083/FBL27119

Original Research

Proteomic Screening of Early Reperfusion in Acute Ischemic Heart and Insights into Mitochondrial-Associated Cell Damage: Role of RIP3

Andrea Marciníková[1,†], Csaba Horváth[1,†], Izabela Jarabicová[1], Petra Majerová[2], Dominika Olešová[2,3], M. Saadeh Suleiman[4], Adriana Adameová[1,5,*]

[1]Department of Pharmacology and Toxicology, Faculty of Pharmacy, Comenius University in Bratislava, 83232 Bratislava, Slovakia
[2]Institute of Neuroimmunology, Slovak Academy of Sciences, 84104 Bratislava, Slovakia
[3]Institute of Experimental Endocrinology, Biomedical Research Center, Slovak Academy of Sciences, 84104 Bratislava, Slovakia
[4]Faculty of Health Sciences, Bristol Heart Institute, The Bristol Medical School, University of Bristol, BS8 1TH Bristol, UK
[5]Centre of Experimental Medicine, Institute for Heart Research, Slovak Academy of Sciences, 81438 Bratislava, Slovakia
*Correspondence: adriana.duris.adameova@uniba.sk (Adriana Adameová)
[†]These authors contributed equally.

Academic Editors: Ramoji Kosuru and Rajesh Katare
Submitted: 24 October 2024 Revised: 5 December 2024 Accepted: 26 December 2024 Published: 24 January 2025

Abstract

Background: Regulated forms of necrosis-like cell death (e.g., necroptosis) have been shown to contribute to cardiac ischemia/reperfusion (I/R) injury. However, pro-inflammatory necroptosis is unlikely to be involved during early reperfusion and little is known about the associated molecular changes. Thus, this study aimed to provide an in-depth protein screening with a particular focus on pro-pyroptotic and mitochondrial damage-related pathways. **Methods**: Langendorff-perfused rat hearts were subjected to 30-minute global ischemia followed by 10-minute reperfusion. Liquid chromatography coupled with mass spectrometry (LC-MS/MS) and immunoblotting techniques were used to study the complex cardiac proteome. In addition, calcium-induced mitochondrial swelling and lactate dehydrogenase (LDH) release were examined to assess mitochondrial stress and necrosis phenotype, respectively. **Results**: Approximately 160 proteins linked to cell death signaling, cellular metabolism, and post-translational modifications were significantly differentially expressed in I/R hearts compared to controls. Conventional proteins of pyroptosis, either of canonical or non-canonical signaling, were not affected during the short reperfusion. Notably, this type of I/R was associated with increased expression of p25 cleaved form of poly [ADP-ribose] polymerase 1 (PARP1 p25) and mature apoptosis-inducing factor (AIF), alongside nitrosative stress and mitochondrial swelling. Conversely, a receptor-interacting protein kinase 3 (RIP3) inhibitor (GSK′872, 250 nM) reversed mitochondrial swelling and plasma membrane rupture and mitigated the increase in the expression of PARP1 p25 and AIF. **Conclusions**: This study shows for the first time that necrosis-like injury during early I/R of the isolated heart is associated with mitochondrial events, rather than pro-inflammatory pyroptotic cell death. Furthermore, the inhibition of RIP3 mitigates this injury independent of targeting pro-inflammatory signaling.

Keywords: cell death; inflammation; myocardial ischemia/reperfusion; pyroptosis; receptor-interacting protein kinase 3 inhibition

1. Introduction

Myocardial ischemia/reperfusion (I/R) injury is a complex of various cellular, molecular, and metabolic changes that trigger events such as calcium overload, adenosine triphosphate (ATP) depletion, overproduction of reactive oxygen species and protein synthesis suppression some of which can trigger the opening of the mitochondrial permeability transition pore [1,2]. Collectively, they result in the death of cardiac cells, impair heart function and result in the development of heart failure over time [3].

Although early research indicated only apoptosis and spontaneous necrosis to be involved in myocardial I/R injury, recent findings highlight the role of programmed necrosis-like cell death modes, such as necroptosis, pyroptosis, ferroptosis, parthanatos, and neutrophil extracellular traps-(NET)osis [1,4,5]. Although all these regulated necrosis cell death forms differ in the activation and execution mechanisms, their common feature is the rupture of the plasma membrane [6].

Pyroptosis can proceed through canonical (inflammasome-related), non-canonical (inflammasome-independent), and alternative axes [7]. Upon the initiation of canonical pyroptotic death, the protein expression of nucleotide-binding domain leucine-rich-containing family (NLRC), pyrin domain-containing-3 (NLRP3), NLRC4 or absent in melanoma 2 (AIM2) increases. Their increase leads to their oligomerisation and assembly with apoptosis-associated speck-like protein (ASC) and pro-caspase-1, finally forming the NLRP3, NLRC4 or AIM2 inflammasome, respectively. Additionally, activated caspase-1 cleaves gasdermin D (GSDMD) releasing its cytotoxic N-terminal (GSDMD-NT) fragment which can oligomerize and translocate to the plasma membrane causing disruption to the membrane. Caspase-1 also leads to the

production of interleukin-1β (IL-1β), a pro-inflammatory cytokine, which is released into the extracellular space via the GSDMD-NT pores [7,8]. Under conditions of non-canonical pyroptosis, the activation of GSDMD occurs by caspase-11 (alternatively, by caspase-4/5 in humans) independently of the inflammasomes [7,9]. Although very little is known about the alternative pathways of pyroptosis, it is obvious that such signaling involves pro-apoptotic caspases (caspase-3 and -8) or mitochondria-related activation of GSDMD or other gasdermins, such as gasdermin C (GSDMC) or gasdermin E (GSDME) [7].

In an earlier study, we showed that necrosis-like cell death is likely to be responsible for the damage during 10-minute reperfusion in the isolated Langendorff-perfused rat hearts [10]. Because necroptosis has not been proven as a predominant form of regulated necrosis under such conditions, we aimed to further explore potential pyroptotic mechanisms. We evaluated canonical, non-canonical and alternative signaling pathways of pyroptosis and possible mitochondrial cell death-associated events that might be involved in promoting both these processes. In addition, we carried out a detailed liquid chromatography coupled with mass spectrometry (LC-MS/MS) protein screening to provide a more comprehensive protein profile and to uncover other potential mechanisms involved.

2. Materials and Methods

2.1 Animals and Experimental Design

Approval for the study was granted by the Animal Welfare Ethical Review Board at the University of Bristol (ethical approval number UB/15/017). Procedures adhered to the Guide for the Care and Use of Laboratory Animals issued by the US National Institutes of Health (Guide, NRC 2011) and complied with the UK's Animals Act of 1986 [11]. Adult male Wistar rats (14–16 weeks old; 250–260 g) were provided by Charles River Laboratories (Oxford, UK). The animals were acclimatised in a controlled environment (23 $\pm$ 1 °C, 60–70% humidity, 12-h light/dark cycle) with unrestricted access to water and standard rat chow for a duration of 4–7 days. Following acclimation, the rats were terminated through stunning followed by cervical dislocation, and the hearts were quickly harvested, rinsed in ice-cold perfusion buffer and retrograde perfused in Langendorff mode as per established protocols [10]. The hearts were randomly assigned to one of three groups: Control, perfusion-only (n = 6), or Ischemia/Reperfusion (I/R) (n = 7), where global ischemia was induced by aortic flow occlusion for 30 minutes, succeeded by a 10-minute reperfusion phase. An additional group underwent I/R and was treated with the receptor-interacting protein kinase 3 (RIP3) inhibitor GSK′872 (250 nM) (S8465, Selleck Chemicals, Pittsburgh, PA, USA) throughout the reperfusion period (I/R+GSK′872) (n = 7) [10]. After the experimental procedure, ventricular tissues were swiftly homogenised for mitochondria isolation. Left ventricular samples were also collected, frozen in liquid nitrogen and stored at –80 °C for later molecular analyses.

2.2 Liquid Chromatography with Mass Spectrometry (LC-MS/MS) Analysis

Heart tissues were homogenised in a lysis buffer comprising 200 mM Tris, 150 mM NaCl, 1 mM ethylenediaminetetraacetic acid (EDTA), 1 mM sodium orthovanadate (Na3VO4), 20 mM sodium fluoride (NaF), 0.5% Triton X-100 (pH 7.4) (Sigma-Aldrich, MO, USA), and a complete protease inhibitor cocktail (Roche, Mannheim, Germany). Protein precipitate was achieved overnight using 80% ice-cold acetone (Sigma-Aldrich, MO, USA). Following centrifugation, the pellets were solubilised in 8 M urea (Sigma-Aldrich, MO, USA). Protein concentrations were quantified using the Bio-Rad protein assay (Bio-Rad Laboratories GmbH, Colbe, Germany). A total of 100 µg of protein was reduced with 10 mM dithiothreitol (Sigma-Aldrich, MO, USA) in 100 mM ammonium bicarbonate (Sigma-Aldrich, MO, USA) at 37 °C for one hour. Alkylation was conducted using 15 mM iodoacetamide (Sigma-Aldrich, MO, USA) in 100 mM ammonium bicarbonate, protected from light for 30 minutes. Trypsin digestion (Promega, Wisconsin, USA) was performed at an enzyme-to-substrate ratio of 1:100 for overnight incubation at 37 °C. The resulting peptide mixtures (100 ng) were separated by Acquity M-Class Ultra-High-Performance Liquid Chromatography (Waters, Milford, MA, USA), utilising a nanoEase Symmetry C18 trap column (25 mm length, 180 µm diameter, 5 µm particle size) (Waters, Milford, MA, USA) for desalting before transferring to a nanoEase High Strength Silica T3 C18 analytical column (100 mm length, 75 µm diameter, 1.8 µm particle size). A 90-minute gradient of acetonitrile (5% to 35%) (Sigma-Aldrich, MO, USA) with 0.1% formic acid (Sigma-Aldrich, MO, USA) was applied at a flow rate of 300 nL/minute. The analysis was performed using a Synapt G2-Si quadrupole time-of-flight mass spectrometer with ion mobility (Waters, Milford, MA, USA). Data were captured in a data-independent fashion while maintaining a spectral acquisition rate of one second. Peak detection and processing were executed using Progenesis QI 4.0 software (Waters, Milford, MA, USA). Calibration and normalisation of peak intensities were based on median distribution [12].

2.3 Measurement of Lactate Dehydrogenase Activity

The activity of lactate dehydrogenase (LDH) was assessed by analysing the effluent collected from both groups during the entirety of the 10-minute reperfusion [10]. Samples were mixed with a buffer containing 100 mM triethanolamine and 100 µM reduced beta-nicotinamide adenine dinucleotide (β-NADH), followed by the addition of 0.1 M sodium pyruvate. The absorbance at 340 nm (A340) was monitored using a spectrophotometer over 5 minutes at 37 °C.

2.4 Mitochondrial Fraction Isolation and Assessment of Mitochondrial Swelling

The mitochondrial fraction was isolated in accordance with previously established protocols [10]. Ventricular tissue was placed in chilled sucrose buffer consisting of 300 mM sucrose, 10 mM Tris-HCl, 1 mM ethylene glycol bis (2-aminoethyl ether)-N,N,N′,N′-tetraacetic acid (EGTA) (pH = 7.2) (Sigma-Aldrich, MO, USA) and thoroughly homogenized. The resulting homogenate was quickly diluted with an isolation buffer containing 5 mg/mL bovine serum albumin (Sigma-Aldrich, MO, USA) and centrifuged at 2000 ×g for 2 minutes to eliminate cellular debris. The supernatant was then subjected to a second centrifugation at 10,000 ×g for 5 minutes to collect a crude particulate fraction, which was then re-suspended in the isolation buffer mentioned above. This mixture underwent further centrifugation at 10,000 ×g for another 5 minutes to obtain a pellet representing the mitochondrial fraction. This pellet was subsequently re-suspended in the isolation buffer for the assessment of mitochondrial swelling. This measurement was conducted at 37 °C under de-energized conditions by observing the reduction in light scattering, quantified as A520, in line with prior methodologies [10]. Mitochondrial swelling was induced by introducing 1 mM of calcium chloride ($CaCl_2$), resulting in a free buffered [Ca^{2+}] of 80 µM [13]. This phenomenon is associated with the mitochondrial permeability transition pore opening, which can be inhibited by cyclosporin A [14,15].

2.5 SDS-PAGE and Immunoblotting

For immunoblotting assessment, left ventricular tissues were prepared using sodium dodecyl sulphate-polyacrylamide gel electrophoresis (SDS-PAGE) and Western blotting techniques as previously documented [10]. Briefly, after electrophoresis, proteins were transferred onto polyvinylidene fluoride (PVDF) membranes (Immobilon-P, Merck Millipore) and incubated with various primary antibodies, including apoptosis-inducing factor (AIF) (#4642, Cell Signaling Technology, Danvers, MA, USA), AIM2 (ab119791, Abcam, Cambridge, UK), caspase-1 (ab179515, Abcam, Cambridge, UK), Caspase-11 (#14340, Cell Signaling Technology, Danvers, MA, USA), Caspase-3 (#9662, Cell Signaling Technology, Danvers, MA, USA), Caspase-8 (#4790, Cell Signaling Technology, Danvers, MA, USA), CypD (# 78247, Cell Signaling Technology, Danvers, MA, USA), GSDMC (ab225635, Abcam, Cambridge, UK), GSDMD (#46451, Cell Signaling Technology, Danvers, MA, USA), GSDME (#88874, Cell Signaling Technology, Danvers, MA, USA), IL-1β (ab9722, Abcam, Cambridge, UK), IL-33 (ab187060, Abcam, Cambridge, UK), inducible nitric oxide synthase (iNOS) (610432, BD Biosciences, Milpitas, CA, USA), NLRC4 (ab201792, Abcam, Cambridge, UK), NLRP3 (ab263899, Abcam, Cambridge, UK), PARP1 p25 (ab32064, Abcam, Cambridge, UK) and tumour necrosis factor (TNF) (ab66579, Abcam, Cambridge, UK). Following this, the membranes were incubated with Horseradish Peroxidase (HRP)-conjugated secondary antibodies: donkey anti-rabbit IgG (711-035-152, Jackson ImmunoResearch, West Grove, PA, USA), donkey anti-mouse IgG (115-035-174, Jackson ImmunoResearch, West Grove, PA, USA), donkey anti-rat IgG (112-035-175, Jackson ImmunoResearch, West Grove, PA, USA) and mouse anti-rat light chain specific IgG-HRP (112-035-175, Jackson ImmunoResearch, West Grove, PA, USA). Protein nitration was evaluated directly (35 µg protein/lane) without additional processing steps using a specific anti-NO2Tyr antibody (#9691, Cell Signaling Technology, Danvers, MA, USA) on a PVDF membrane. Whole-lane signal positivity was then used to calculate the relative expression of modified protein residues vs. the control group. Signals were detected using enhanced chemiluminescence (Crescendo Luminata, Merck Millipore, Burlington, MA, USA) and captured by a chemiluminescence imaging system (myECL imager, Thermo Scientific, Waltham, MA, USA). The positivity of signals across the whole lane was utilised to calculate the relative expression of modified protein residues compared to the control group. Detection of signals was accomplished through enhanced chemiluminescence (Crescendo Luminata, Merck Millipore, Burlington, MA, USA) captured by a chemiluminescence imaging system (myECL imager, Thermo Scientific, Waltham, MA, USA). Total protein staining with Ponceau S, assessed via scanning densitometry, served as the loading control for total tissue lysates [16]. The relative expression of target protein bands of interest was determined by adjusting the intensity against the overall lane protein staining.

2.6 Statistical Analysis

Data are reported as means ± standard error of means (SEM) corresponding to the number of animals per group, while potential outliers were identified and removed from the statistical analyses by utilising Grubbs' test. To evaluate

Table 1. Lactate dehydrogenase (LDH) activity (expressed as AUC) and the extent of mitochondrial swelling in the left ventricles.

Group	Maximal mitochondrial swelling [A520 × 103]	LDH release [AUC]
C	44.21 ± 11.31	83.68 ± 53.82
I/R	78.24 ± 23.44 *	1148 ± 308.1 *
I/R + GSK′872	44.18 ± 12.73 #	637.4 ± 316.2 *#

Control (C), untreated ischemic/reperfused hearts (I/R), and receptor-interacting protein kinase 3 (RIP3) inhibitor-treated hearts (I/R+GSK′872). AUC, area under the curve. Data are presented as mean ± SEM; * $p < 0.05$ vs. C group; # $p < 0.05$ vs. I/R group.

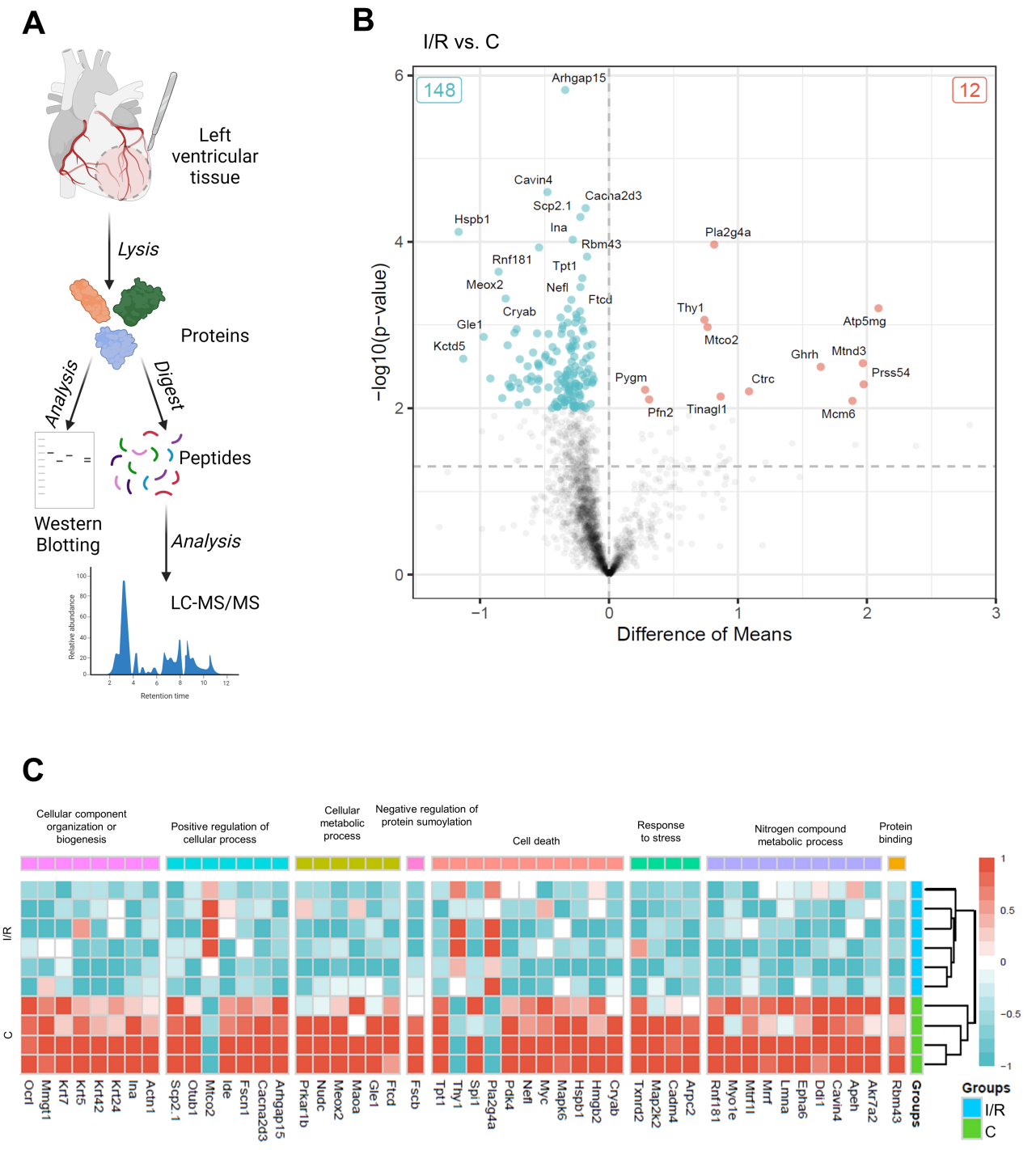

Fig. 1. Liquid chromatography with mass spectrometry (LC-MS/MS) proteome analysis. (A) Schematic representation of proteomic workflow; (B) Volcano plots comparing protein levels between C and I/R groups (significantly differentially expressed proteins were defined with |fold-change| >1.5 and $p < 0.01$); (C) Heatmap illustrating the differentially expressed proteins enriched in C and I/R groups. C, control group; I/R, ischemia/reperfusion group. Created with BioRender.com.

differences between the groups with normally distributed variables, a Student's *t*-test or one-way analysis of variance (ANOVA) with Tukey's post-hoc test was employed. All statistical evaluations were conducted using GraphPad Prism 10.0 for Windows (GraphPad Software, San Diego, CA, USA). Differences between groups were considered significant when $p < 0.05$.

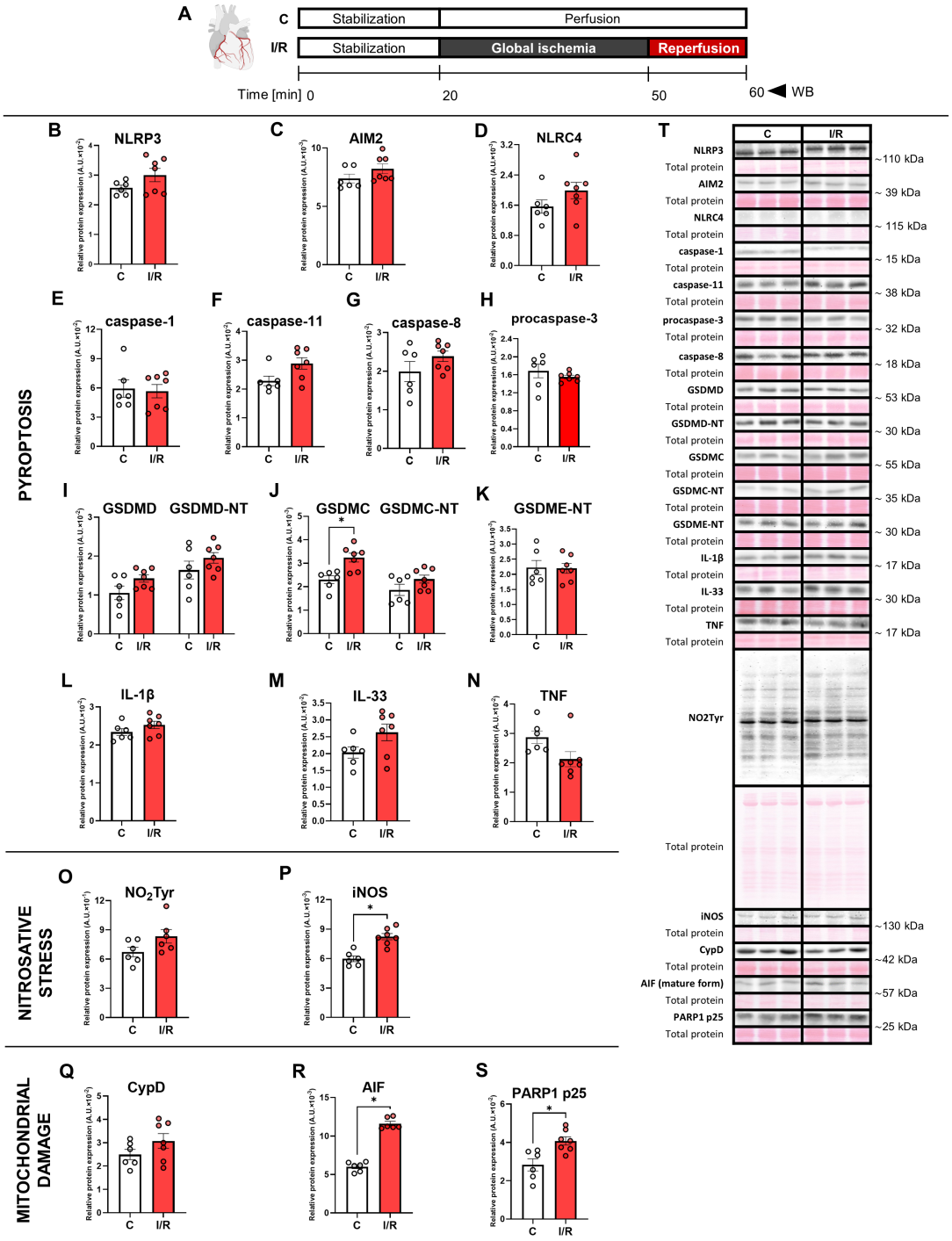

Fig. 2. Analysis of inflammasomes and signalling pathways leading to pyroptosis, nitrosative stress and mitochondrial damage in left ventricles lysates. (A) Schematic representation of the experimental protocol; Immunoblot quantification of (B) NLR family pyrin domain containing 3 (NLRP3); (C) Absent in melanoma 2 (AIM2); (D) NLR family CARD domain-containing 4 (NLRC4); (E) Caspase-1; (F) Caspase-11; (G) Caspase-8; (H) Procaspase-3; (I) Gasdermin D (GSDMD) and N-terminal GSDMD (GSDMD-NT); (J) Gasdermin C (GSDMC) and N-terminal GSDMC (GSDMC-NT); (K) N-terminmal gasdermin E (GSDME-NT); (L) Interleukin-1 beta (IL-1β); (M) Interleukin-33 (IL-33); (N) Tumor necrosis factor (TNF); (O) 3-nitrotyrosine (NO2Tyr); (P) Inducible nitric oxide synthase (iNOS); (Q) Cyclophilin D (CypD); (R) Apoptosis-inducing factor (AIF); (S) p25 cleaved form of poly [ADP-ribose] polymerase 1 (PARP1 p25); (T) Representative immunoblots and total protein staining. C, control group; I/R, ischemia/reperfusion group. Data are presented as mean $\pm$ SEM; * $p < 0.05$. WB, western blot.

In the case of the proteomic analysis, significance ($p < 0.01$) (Fig. 1) was identified using a two-sided *t*-test. A heatmap displaying the top 50 differentially expressed proteins was generated utilising the tidyheatmaps package in R (https://www.r-project.org, v 4.3.1) [12].

3. Results

3.1 LDH Activity and Mitochondrial Swelling

In the first 10 minutes of reperfusion, the LDH activity in the effluent was significantly increased, indicating a necrosis-like phenotype of cardiac damage. Likewise, the maximal extent of mitochondrial swelling as a marker of mitochondrial damage (sensitivity to Ca^{2+}) was higher due to I/R. However, RIP3 inhibition significantly decreased LDH release and inhibited I/R-induced mitochondrial swelling (Table 1).

3.2 Proteomic Analysis

A liquid chromatography coupled with mass spectrometry (LC-MS/MS)-based untargeted proteomics approach identified 160 significantly ($p < 0.01$) altered protein levels between the I/R and control (C) groups. More specifically, 12 proteins were significantly upregulated and 148 downregulated due to 10-minute reperfusion of previously ischemic hearts. Subsequently, group GO analysis was performed and the 50 most significantly altered proteins were categorised into a heatmap based on their involvement in a specific biological process (Fig. 1), such as cell death (GO:0008219), cellular component organisation or biogenesis (GO:0071840), cellular metabolic process (GO:0044237), negative regulation of protein sumoylation (GO:0033234), nitrogen compound metabolic process (GO:0006807), positive regulation of cellular process (GO:0048522), protein binding (GO:0005515), and response to stress (GO:0006950) (Fig. 1). The biological functions and biological action of the most changed proteins being related to cell death are indicated in Table 2 (Ref. [17]). Of note, none of this protein is a conventional protein of the signaling pathway of either of necrosis-like cell death modes.

3.3 Immunoblotting Analysis

3.3.1 Inflammasome Activation and Pyroptosis

The protein expression of the main inflammasome components, NLRP3, absent in melanoma 2 (AIM2) and NLRC4, was unaffected, indicating no involvement in acute I/R injury. Furthermore, there were no changes in the expression of the main pro-pyroptotic caspases, caspase-1 and caspase-11, nor in the expression of caspases associated with both pyroptotic and apoptotic signalling, caspase-8 and pro-caspase 3. The active caspase-3 was fully absent. With the exception of the I/R-mediated upregulation in the total GSDMC level, there were no changes in the expression of other investigated gasdermins, namely GSDMD and GSDME, including their active forms. We also found no I/R-mediated changes in the cleavage of pyroptosis-related IL-1β. Similarly, the proinflammatory interleukin-33 (IL-33) level was comparable in both the control and I/R groups. Interestingly, there was a trend of a decrease ($p = 0.0522$) in the expression of the active fragment of tumour necrosis factor (TNF) in the I/R group (Fig. 2).

3.3.2 Nitrosative Stress

Because mitochondrial damage is associated with nitrogen species production and uncoupled nitric oxide synthase [18], we evaluated the protein tyrosine nitration and the expression of inducible NO synthase (iNOS). Although protein tyrosine nitration was unchanged, iNOS expression was significantly increased due to I/R (Fig. 2).

3.3.3 Markers Associated with Mitochondrial Damage

There were no changes in the expression of cyclophilin D (CypD), a significant regulator of mitochondrial permeability transition pore (mPTP) opening [19], among the groups. However, an increase in mPTP sensitivity to Ca^{2+} (cell swelling) is an important factor in mediating cell death. The levels of the active 57-kDa fragment of apoptosis-inducing factor (AIF), known to be translocated within mitochondria [20] and the p25 fragment of poly (adenosine diphosphate-ribose) polymerase 1 (PARP1) were significantly upregulated in the I/R group (Fig. 2).

3.3.4 Effect of RIP3 Inhibition on I/R Injury and Protein Expression

Since RIP3 inhibition is able to ameliorate the I/R-mediated increase in both the maximal extent of mitochondrial swelling and LDH release (Table 1), we next investigated the associated underlying mechanisms. We found that the RIP3 inhibitor GSK′872 suppressed the I/R-induced increase in the active fragment of AIF and PARP1 p25 expression despite no effect on the CypD levels (Fig. 3).

4. Discussion

This study aimed to provide in-depth protein analysis with a particular focus on pyroptosis and mitochondria-related damage measured during early reperfusion following global ischemia. LC-MS/MS-based proteomic screening has revealed 160 differentially expressed proteins due to 30-minute ischemia and 10-minute reperfusion. There were changes in proteins involved in the signaling of cell death, cellular metabolism, and post-translational modifications. Since the activity of LDH, arguing for the pro-necrotic plasma membrane disruption was increased, we were primarily interested in proteins mediating necrosis-like cell death. However, this detailed untargeted protein approach did not indicate alterations in the most common proteins of necrosis-like regulated forms of cell death. Instead, there were changes in the regulators of other signaling pathways that are linked to cell death. Further blotting

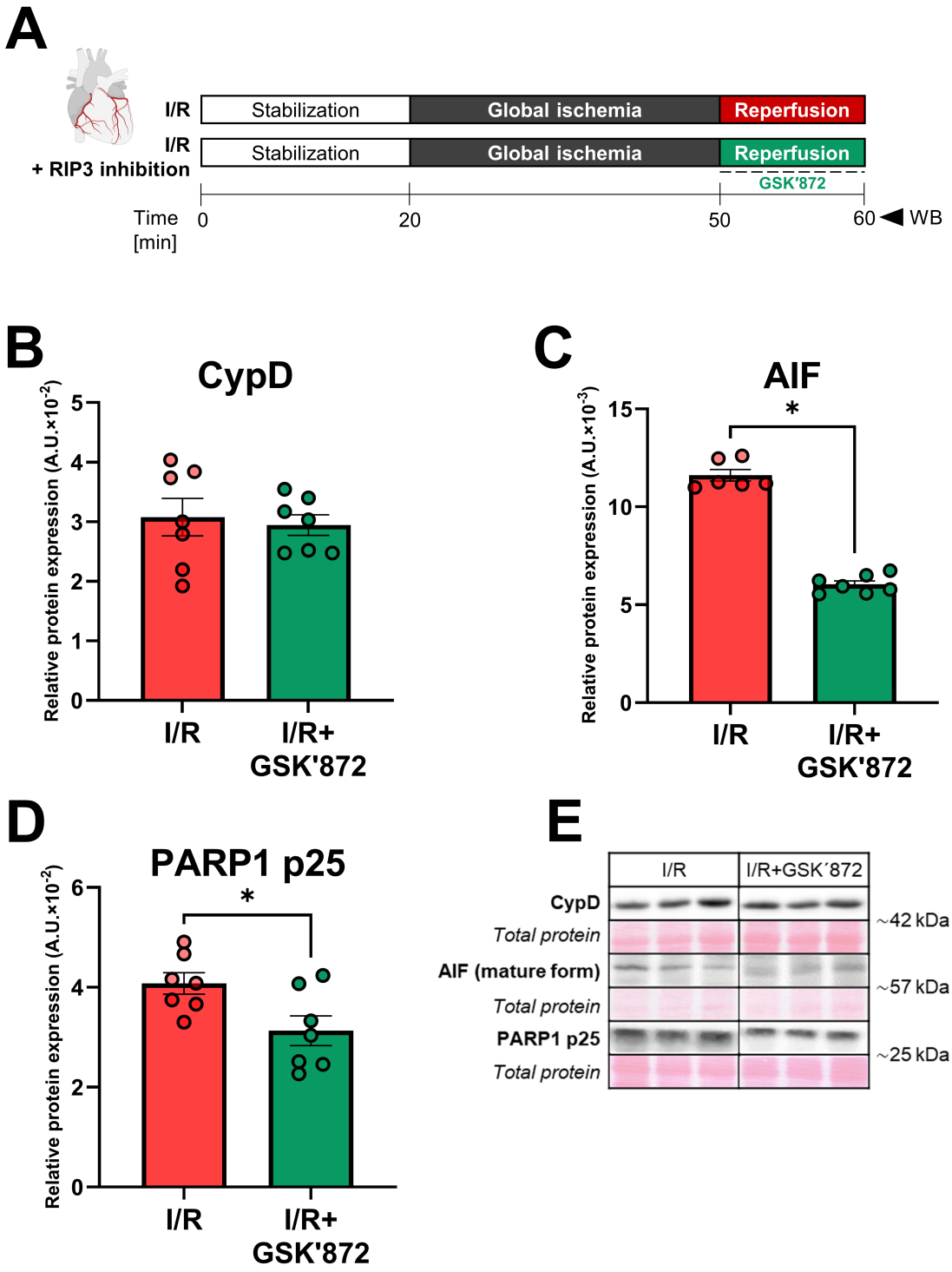

Fig. 3. Analysis of molecules associated with mitochondrial damage in left ventricles and the effect of RIP3 inhibition. (A) Schematic representation of experimental protocol. Immunoblot quantification of (B) CypD, (C) AIF (mature form), (D) PARP1 p25; (E) Representative immunoblots and total protein staining. C, control group; I/R, ischemia/reperfusion group; I/R+GSK′872, ischemia/reperfusion + RIP3 inhibition group. Data are presented as mean ± SEM; * $p < 0.05$.

analysis showed no changes in the expression of pyroptosis-mediating proteins (Fig. 4). Indeed, neither inflammasome-dependent nor independent signalling of pyroptosis was activated. On the other hand, unlike control hearts, the I/R hearts exhibited increased mitochondrial swelling and up-regulated protein expression of AIF and PARP1 p25. Additionally, even though mitochondrial and nitrosative stress were shown to be intertwined, protein tyrosine nitration

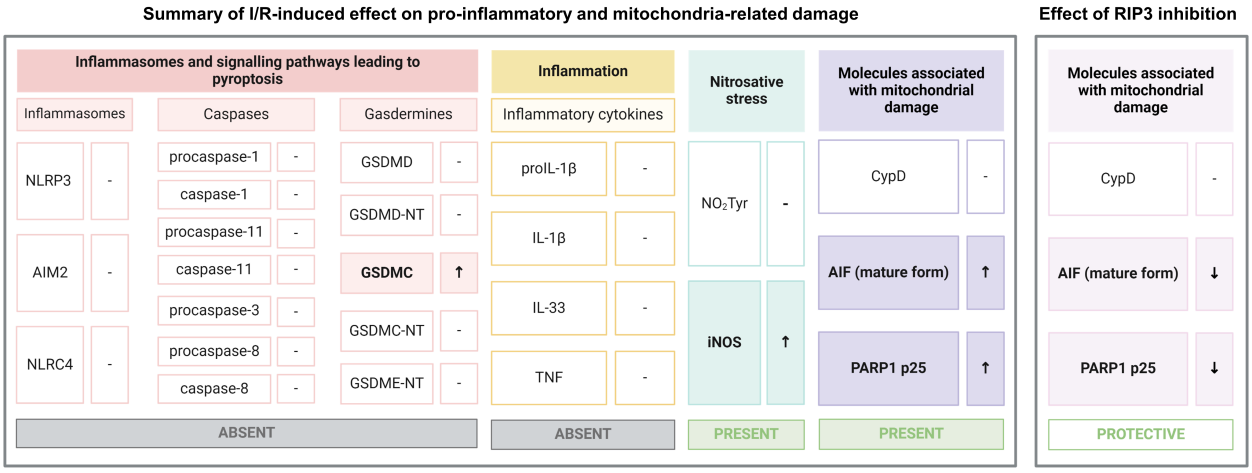

Fig. 4. Summary of main findings on pyroptotic, pro-inflammatory and mitochondria-related events due to early reperfusion and the effect of RIP3 inhibition. Symbols: "-", no statistically significant change in protein expression compared to the control group; "↑", significantly increased ($p < 0.05$) protein expression compared to the control group; "↓", significantly decreased ($p < 0.05$) protein expression compared to the ischemia/reperfusion group.

was unchanged due to I/R. The uncoupled NO signalling likely plays a role under such acute I/R protocol, evidenced by increased iNOS expression (Fig. 4). Importantly, RIP3 inhibition, which has exhibited the capability to prevent I/R-induced mitochondrial swelling and plasma membrane disruption [10], attenuated these mitochondrial alterations, thereby highlighting an interlink between RIP3, mitochondrial events and associated necrosis-like cell death (Fig. 4).

Pyroptosis has been studied in myocardial I/R injury in models of *in vivo* [21–23], as well as under conditions outside of the living organism, *in vitro* isolated myocardial cells [24,25], and *ex vivo* hearts [26,27]. Here, we used a model of short reperfusion of previously ischemic Langendorff-perfused hearts in order to examine whether the very first minutes are critical for pyroptosis signalling because necroptosis was unlikely activated under such conditions [10]. The expression of the main pro-pyroptotic inflammasomes such as NLRP3, NLRC4 and AIM2 was unchanged which is in contrast with the studies employing a longer reperfusion phase (20 minutes–24 hours) [26–32]. Likewise, the downstream markers of both canonical and non-canonical pyroptosis, including caspase-1, caspase-11, GSDMD, IL-1β, and IL-33, were unlikely to be modified under such experimental conditions. Similarly, we found no significant increase in the expression of TNF, another endogenous inducible damage-associated molecular pattern (DAMP) that can activate programmed necrosis-like cell death [33]. It is important to note that an increase in NLRP3, caspase-1, IL-1β and TNF was reported in studies employing a longer reperfusion phase, ranging from 20 minutes to 2 hours [26,27]. Furthermore, the 10-minute acute reperfusion in this study could not activate the alternative pyroptotic pathway. Although total GSDMC expression was increased, its N-terminal fragment and upstream target, caspase-8, did not change. Interestingly, the cleaved form of caspase-3 and the total form of GSDME were not detected; however, neither the zymogen form of this caspase, procaspase-3, nor NT-GSDME were found to be altered due to I/R. It is plausible that changes in the expression of the caspases-3/8 and GSDME/GSDMC might occur during prolonged reperfusion comparably to the changes in canonical pyroptotic proteins [25,34–36]. Available literature provides limited information on molecular mechanisms of GSDMC and GSDME in pyroptosis during myocardial I/R injury.

From the aforementioned discussion, the observed necrosis-like injury of the heart during the first minutes of reperfusion is unlikely to be due to intracardiac signalling of pyroptosis and potentially originates from other mechanisms. Thus, to address this issue we looked at mitochondria-associated pro-death events. We evaluated mitochondrial swelling, nitrosative stress, CypD, PARP1 p25 and AIF expression. Tyrosine nitration and CypD levels were not changed due to I/R, whereas we showed up-regulation of iNOS, PARP1 p25 and AIF after 10-minute reperfusion. In line with our data, the increase in iNOS and AIF was also found in the hearts subjected to the prolonged periods of reperfusion, (90 minutes–2 hours) [37,38]. In these studies employing a model of *ex vivo* perfused hearts, the nuclear fraction of AIF increased, while the mitochondrial fraction decreased. Similar changes in AIF fractions were observed during 3-hour reperfusion under *in vivo* conditions [39]. PARP-1, which seems to exert profound mitochondria-related effects on cellular energetics potentially culminating in cellular demise [40,41], was also reported to be increased after 1–4 hours of *in vivo* reperfusion [41].

Table 2. Molecular functions, biological processes, and related pathways of cell death-related proteins identified by liquid chromatography with mass spectrometry .

Protein	Full protein name	Molecular functions	Biological process and related pathways	UniProt ID
Cryab	Alpha-crystallin B chain	Chaperone-like activity, small heat shock protein.	Negative regulation of reactive oxygen species metabolic process, response to hypoxia, programmed cell death - negative regulation of apoptotic processes.	P23928
HMGB2	High mobility group protein B2	Damaged DNA binding.	Inflammatory response to antigenic stimulus, positive regulation of innate immune response.	P52925
Hspb1	Heat shock protein beta-1	Molecular chaperone, small heat shock protein, cellular component of cardiac myofibril.	Intracellular signal transduction, negative regulation of cellular response to oxidative stress, positive regulation of IL-1β production, positive regulation of TNF production, response to ischemia, stress response.	P42930
Mapk6	Mitogen-activated protein kinase 6	Serine/threonine-protein kinase; transferase.	Intracellular signal transduction.	P27704
Myc	Myc proto-oncogene protein	DNA-binding; glycoprotein; transcription regulation.	Cellular response to cytokine stimulus, cellular response to hypoxia, glucose metabolism process, inner mitochondrial membrane organization, positive regulation of mitochondrial membrane potential, cellular response to hypoxia, immune processes.	P09416
Nefl	Neurofilament light polypeptide	Direct protein sequencing, glycoprotein.	Protein polymerization.	P19527
Pdk4	[Pyruvate dehydrogenase (acetyl-transferring)] kinase isozyme 4, mitochondrial	Cellular component of mitochondrial matrix, protein kinase activity.	Cellular response to starvation, reactive oxygen species metabolic process, regulation of glucose metabolic process, regulation of pH.	O54937
Pla2g4a	Phospholipase A2	Membrane lipid remodelling and biosynthesis of lipid mediators of the inflammatory response.	Response to calcium ion.	F7EZZ6
Spi1	Transcription factor PU.1	DNA-binding; transcription regulation.	Immune system processes, programmed cell death.	Q6BDS1
Thy1	Thy-1 membrane glycoprotein	Cell surface glycoprotein, protein kinase binding.	Cytoskeleton organization, negative regulation of protein kinase activity, positive regulation of release of sequestered calcium ion into cytosol, receptor clustering, immune system processes, programmed cell death, cell-cell signalling, positive regulation of release of sequestered calcium ion into cytosol.	P01830
Tpt1	Translationally controlled tumor protein	Calcium ion binding, DNA-binding transcription factor binding.	Programmed cell death - negative regulation of intrinsic apoptotic signaling pathway in response to DNA damage.	P63029

The table represents the most significantly altered proteins between the control and ischemia/reperfusion groups. Data was acquired from the UniProt database [17]. IL-1β, interleukin-1β; TNF, tumor necrosis factor.

Because RIP3 can act as an upstream protein capable of activating proteins including PARP1 p25 and AIF as well as calcium-sensitive regulation of mPTP opening and thereby producing subsequent mitochondrial swelling and damage [10], we investigated the effect of RIP3 inhibition. We report for the first time that inhibition of RIP3 significantly reduced the expression of PARP1 p25 and mature AIF. As it was accompanied by the mitigation of mitochondrial swelling, it can be suggested that the changes in these proteins might underlie, at least in part, the cardioprotection of a pharmacological approach targeting RIP3. In agreement with our work is a study employing different tissue and a different model of I/R, it has been shown that RIP3 inhibition also significantly limited neuronal death in a potential AIF-dependent manner in global cerebral I/R injury [42].

Study Limitations

While this study provides novel insights into I/R mediated cardiac damage and likely RIP3 involvement in the underlying mechanisms, several limitations should be acknowledged. First, as an *ex vivo* investigation, it captures an ultra-acute state, which may not fully mimic the complexity of *in vivo* conditions or encompass the broader spectrum of clinical scenarios. Additionally, the findings are predominantly derived from SDS-PAGE/Western Blot analyses, which, while informative, do not enable precise localisation or identification of the specific cardiac cell types affected.

Another limitation is the use of a single dose of the RIP3 inhibitor (GSK′872). Moreover, the study would have benefited from complementary approaches, such as employing genetic knockout models, to provide more comprehensive mechanistic insights. These limitations underscore the need for further research to validate and expand upon the current findings.

5. Conclusions

Collectively, the data from this and our previous study [10] suggest that early minutes of reperfusion of the isolated hearts lead to the plasma membrane rupture that is not due to necroptotic nor pyroptotic cell death and that non-inflammatory, mitochondrial RIP3-mediated mechanisms might underlie the myocardial damage. Further studies are needed to examine the participation of RIP3 in such PARP1 p25 and AIF changes and the relevance of RIP3 inhibition as a novel cardioprotective strategy for acute I/R-associated events.

Availability of Data and Materials

The data that support the findings of this study are available from the corresponding author upon reasonable request.

Author Contributions

Conceptualisation—AA; methodology—AM, CH, IJ, PM, DO, MSS; writing- original draft preparation—AM, CH, AA; writing- review and editing—AM, AA, CH, IJ, MSS; supervision—AA; interpretation of data for the work—AM, CH, MSS, AA. All authors contributed to editorial changes in the manuscript. All authors read and approved the final manuscript. All authors have participated sufficiently in the work and agreed to be accountable for all aspects of the work.

Ethics Approval and Consent to Participate

Approval for the study was granted by the Animal Welfare Ethical Review Board at the University of Bristol (ethical approval number UB/15/017). Procedures adhered to the Guide for the Care and Use of Laboratory Animals issued by the US National Institutes of Health (Guide, NRC 2011) and complied with the UK's Animals Act of 1986.

Acknowledgment

The figures in this manuscript were created with BioRender.com. URL: https://www.biorender.com/.

Funding

This research was funded by grants VEGA 1/0078/25, VEGA 1/0016/20, APVV-20-0242, UK/1181/2024 and the EU Next Generation EU through the Recovery and Resilience Plan for Slovakia under the project No. 09I03-03-V04-00231.

Conflict of Interest

The authors declare no conflict of interest.

References

[1] Heusch G. Myocardial ischemia/reperfusion: Translational pathophysiology of ischemic heart disease. Med (New York, N.Y.). 2024; 5: 10–31. https://doi.org/10.1016/j.medj.2023.12.007.

[2] Perrelli MG, Pagliaro P, Penna C. Ischemia/reperfusion injury and cardioprotective mechanisms: Role of mitochondria and reactive oxygen species. World Journal of Cardiology. 2011; 3: 186–200. https://doi.org/10.4330/wjc.v3.i6.186.

[3] Soares ROS, Losada DM, Jordani MC, Évora P, Castro-E-Silva O. Ischemia/Reperfusion Injury Revisited: An Overview of the Latest Pharmacological Strategies. International Journal of Molecular Sciences. 2019; 20: 5034. https://doi.org/10.3390/ijms20205034.

[4] Zhang J, Liu D, Zhang M, Zhang Y. Programmed necrosis in cardiomyocytes: mitochondria, death receptors and beyond. British journal of pharmacology. 2019; 176: 4319–4339. https://doi.org/10.1111/bph.14363.

[5] Mishra PK, Adameova A, Hill JA, Baines CP, Kang PM, Downey JM, *et al*. Guidelines for evaluating myocardial cell death. American journal of physiology. Heart and circulatory physiology. 2019; 317: H891–H922. https://doi.org/10.1152/ajpheart.00259.2019.

[6] Feoktistova M, Leverkus M. Programmed necrosis and necrop-

tosis signalling. The FEBS Journal. 2015; 282: 19–31. https://doi.org/10.1111/febs.13120.

[7] Yu P, Zhang X, Liu N, Tang L, Peng C, Chen X. Pyroptosis: mechanisms and diseases. Signal transduction and targeted therapy. 2021; 6: 128. https://doi.org/10.1038/s41392-021-00507-5.

[8] Bergsbaken T, Fink SL, Cookson BT. Pyroptosis: host cell death and inflammation. Nature reviews. Microbiology. 2009; 7: 99–109. https://doi.org/10.1038/nrmicro2070.

[9] Broz P, Pelegrín P, Shao F. The gasdermins, a protein family executing cell death and inflammation. Nature Reviews. Immunology. 2020; 20: 143–157. https://doi.org/10.1038/s41577-019-0228-2.

[10] Horvath C, Young M, Jarabicova I, Kindernay L, Ferenczyova K, Ravingerova T, *et al*. Inhibition of Cardiac RIP3 Mitigates Early Reperfusion Injury and Calcium-Induced Mitochondrial Swelling without Altering Necroptotic Signalling. International Journal of Molecular Sciences. 2021; 22: 7983. https://doi.org/10.3390/ijms22157983.

[11] Percie du Sert N, Hurst V, Ahluwalia A, Alam S, Avey MT, Baker M, *et al*. The ARRIVE guidelines 2.0: Updated guidelines for reporting animal research. PLoS Biology. 2020; 18: e3000410. https://doi.org/10.1371/journal.pbio.3000410.

[12] Mangiola S, Papenfuss AT. tidyHeatmap: an R package for modular heatmap production based on tidy principles. Journal of Open Source Software. 2020; 5: 2472. https://doi.org/10.21105/joss.02472.

[13] Khaliulin I, Parker JE, Halestrap AP. Consecutive pharmacological activation of PKA and PKC mimics the potent cardioprotection of temperature preconditioning. Cardiovascular Research. 2010; 88: 324–333. https://doi.org/10.1093/cvr/cvq190.

[14] Suleiman MS, Halestrap AP, Griffiths EJ. Mitochondria: a target for myocardial protection. Pharmacology & Therapeutics. 2001; 89: 29–46. https://doi.org/10.1016/s0163-7258(00)00102-9.

[15] Khaliulin I, Halestrap AP, Bryant SM, Dudley DJ, James AF, Suleiman MS. Clinically-relevant consecutive treatment with isoproterenol and adenosine protects the failing heart against ischaemia and reperfusion. Journal of Translational Medicine. 2014; 12: 139. https://doi.org/10.1186/1479-5876-12-139.

[16] Moritz CP. Tubulin or Not Tubulin: Heading Toward Total Protein Staining as Loading Control in Western Blots. Proteomics. 2017; 17. https://doi.org/10.1002/pmic.201600189.

[17] UniProt Consortium. UniProt: the Universal Protein Knowledgebase in 2023. Nucleic Acids Research. 2023: 51: D523–D531. https://doi.org/10.1093/nar/gkac1052.

[18] Chen CL, Zhang L, Jin Z, Kasumov T, Chen YR. Mitochondrial redox regulation and myocardial ischemia-reperfusion injury. American journal of physiology. Cell Physiology. 2022; 322: C12–C23. https://doi.org/10.1152/ajpcell.00131.2021.

[19] Nakagawa T, Shimizu S, Watanabe T, Yamaguchi O, Otsu K, Yamagata H, *et al*. Cyclophilin D-dependent mitochondrial permeability transition regulates some necrotic but not apoptotic cell death. Nature. 2005; 434: 652–658. https://doi.org/10.1038/nature03317.

[20] Wang Y, Dawson VL, Dawson TM. Poly(ADP-ribose) signals to mitochondrial AIF: a key event in parthanatos. Experimental Neurology. 2009; 218: 193–202. https://doi.org/10.1016/j.expneurol.2009.03.020.

[21] Toldo S, Mezzaroma E, Van Tassell BW, Farkas D, Marchetti C, Voelkel NF, *et al*. Interleukin-1β blockade improves cardiac remodelling after myocardial infarction without interrupting the inflammasome in the mouse. Experimental Physiology. 2013; 98: 734–745. https://doi.org/10.1113/expphysiol.2012.069831.

[22] Qiu Z, Lei S, Zhao B, Wu Y, Su W, Liu M, *et al*. NLRP3 Inflammasome Activation-Mediated Pyroptosis Aggravates Myocardial Ischemia/Reperfusion Injury in Diabetic Rats. Oxidative Medicine and Cellular Longevity. 2017; 2017: 9743280. https://doi.org/10.1155/2017/9743280.

[23] Lou Y, Wang S, Qu J, Zheng J, Jiang W, Lin Z, *et al*. miR-424 promotes cardiac ischemia/reperfusion injury by direct targeting of CRISPLD2 and regulating cardiomyocyte pyroptosis. International Journal of Clinical and Experimental Pathology. 2018; 11: 3222–3235.

[24] Martinon F, Burns K, Tschopp J. The Inflammasome: a molecular platform triggering activation of inflammatory caspases and processing of proIL-beta. Molecular Cell. 2002; 10: 417–426. https://doi.org/10.1016/s1097-2765(02)00599-3.

[25] Shi H, Gao Y, Dong Z, Yang J, Gao R, Li X, *et al*. GSDMD-Mediated Cardiomyocyte Pyroptosis Promotes Myocardial iR Injury. Circulation Research. 2021; 129: 383–396. https://doi.org/10.1161/CIRCRESAHA.120.318629.

[26] Mastrocola R, Penna C, Tullio F, Femminò S, Nigro D, Chiazza F, *et al*. Pharmacological Inhibition of NLRP3 Inflammasome Attenuates Myocardial Ischemia/Reperfusion Injury by Activation of RISK and Mitochondrial Pathways. Oxidative Medicine and Cellular Longevity. 2016; 2016: 5271251. https://doi.org/10.1155/2016/5271251.

[27] Zhang J, Huang L, Shi X, Yang L, Hua F, Ma J, *et al*. Metformin protects against myocardial ischemia-reperfusion injury and cell pyroptosis via AMPK/NLRP3 inflammasome pathway. Aging. 2020; 12: 24270–24287. https://doi.org/10.18632/aging.202143.

[28] Jorgensen I, Miao EA. Pyroptotic cell death defends against intracellular pathogens. Immunological Reviews. 2015; 265: 130–142. https://doi.org/10.1111/imr.12287.

[29] Miao EA, Rajan JV, Aderem A. Caspase-1-induced pyroptotic cell death. Immunological Reviews. 2011; 243: 206–214. https://doi.org/10.1111/j.1600-065X.2011.01044.x.

[30] Liang J, Wang Q, Li JQ, Guo T, Yu D. Long non-coding RNA MEG3 promotes cerebral ischemia-reperfusion injury through increasing pyroptosis by targeting miR-485/AIM2 axis. Experimental Neurology. 2020; 325: 113139. https://doi.org/10.1016/j.expneurol.2019.113139.

[31] Li XQ, Yu Q, Fang B, Zhang ZL, Ma H. Knockdown of the AIM2 molecule attenuates ischemia-reperfusion-induced spinal neuronal pyroptosis by inhibiting AIM2 inflammasome activation and subsequent release of cleaved caspase-1 and IL-1β. Neuropharmacology. 2019; 160: 107661. https://doi.org/10.1016/j.neuropharm.2019.05.038.

[32] Poh L, Kang SW, Baik SH, Ng GYQ, She DT, Balaganapathy P, *et al*. Evidence that NLRC4 inflammasome mediates apoptotic and pyroptotic microglial death following ischemic stroke. Brain, Behavior, and Immunity. 2019; 75: 34–47. https://doi.org/10.1016/j.bbi.2018.09.001.

[33] Bertheloot D, Latz E, Franklin BS. Necroptosis, pyroptosis and apoptosis: an intricate game of cell death. Cellular & Molecular Immunology. 2021; 18: 1106–1121. https://doi.org/10.1038/s41423-020-00630-3.

[34] Shen S, He F, Cheng C, Xu B, Sheng J. Uric acid aggravates myocardial ischemia–reperfusion injury via ROSNLRP3 pyroptosis pathway. Biomedicine & Pharmacotherapy. 2021; 133: 110990. https://doi.org/10.1016/j.biopha.2020.110990.

[35] Szobi A, Farkašová-Ledvényiová V, Lichý M, Muráriková M, Čarnická S, Ravingerová T, *et al*. Cardioprotection of ischaemic preconditioning is associated with inhibition of translocation of MLKL within the plasma membrane. Journal of Cellular and Molecular Medicine. 2018; 22: 4183–4196. https://doi.org/10.1111/jcmm.13697.

[36] Fauconnier J, Meli AC, Thireau J, Roberge S, Shan J, Sassi Y, *et al*. Ryanodine receptor leak mediated by caspase-8 activation leads to left ventricular injury after myocardial ischemia-reperfusion. Proceedings of the National Academy of Sciences

of the United States of America. 2011; 108: 13258–13263. https://doi.org/10.1073/pnas.1100286108.

[37] Kim G, Chun Y, Park J, Kim M. Role of apoptosis-inducing factor in myocardial cell death by ischemia–reperfusion. Biochemical and Biophysical Research Communications. 2003; 309: 619–624. https://doi.org/10.1016/j.bbrc.2003.08.045.

[38] Kyoi S, Otani H, Matsuhisa S, Akita Y, Enoki C, Tatsumi K, *et al*. Role of oxidative/nitrosative stress in the tolerance to ischemia/reperfusion injury in cardiomyopathic hamster heart. Antioxidants & Redox Signaling. 2006; 8: 1351–1361. https://doi.org/10.1089/ars.2006.8.1351.

[39] Song ZF, Ji XP, Li XX, Wang SJ, Wan SH, Zhang Y. Inhibition of the activity of poly (ADP-ribose) polymerase reduces heart ischaemia/reperfusion injury via suppressing JNK-mediated AIF translocation. Journal of cellular and molecular medicine. 2008; 12; 1220–1228. https://doi.org/10.1111/j.1582-4934.2008.00183.x.

[40] Hong SJ, Dawson TM, Dawson VL. Nuclear and mitochondrial conversations in cell death: PARP-1 and AIF signaling. Trends in Pharmacological Sciences. 2004; 25: 259–264. https://doi.org/10.1016/j.tips.2004.03.005.

[41] Schriewer JM, Peek CB, Bass J, Schumacker PT. ROS-mediated PARP activity undermines mitochondrial function after permeability transition pore opening during myocardial ischemia-reperfusion. Journal of the American Heart Association. 2013; 2: e000159. https://doi.org/10.1161/JAHA.113.000159.

[42] Hu W, Wu X, Yu D, Zhao L, Zhu X, Li X, *et al*. Regulation of JNK signaling pathway and RIPK3/AIF in necroptosis-mediated global cerebral ischemia/reperfusion injury in rats. Experimental Neurology. 2020; 331: 113374. https://doi.org/10.1016/j.expneurol.2020.113374.